

MULTI-SCALE MECHANICAL NUMERICAL ANALYSIS OF MULTI-AXIAL COMPOSITES

Valter Carvelli

Department of Structural Engineering, Technical University (Politecnico) of Milan (Italy)

Keywords: *multi-axial composites, homogenization, finite element method, mechanical features*

Abstract

In this paper an overview of a numerical approach to evaluate the mechanical behaviour until failure of multi-axial composites and the validation of the method against experiments is presented. The procedure is a multi-scale modelling technique essentially based on the solution of nested boundary value problems, one for each scale. The main assumption at each scale is the periodic distribution of the reinforcements to apply the homogenization theory for periodic media.

The modelling is implemented in a two-scale computational homogenization procedure to study the mechanical behaviour of textile composites and multi-layer stitched composites. The experimental data on a glass textile plain weave composite and a multi-axial multi-ply carbon stitched laminate are compared to the results of the numerical analyses.

1 Introduction

Multi-axial composites are obtained as combination of uni-directional plies with transversal consolidation by stitching or by 2D/3D weaved textiles. These techniques allow to better exploit the material properties since a full use of the stiffness and strength of the fibres is possible.

The prediction and/or the evaluation of the mechanical properties of these composite materials are widely important in many industrial fields to design materials and structures.

In this paper a numerical approach to evaluate the mechanical behaviour until failure of multi-axial composites and the validation of the method against experiments (see e.g. [1]) is detailed.

The numerical approach is a multi-scale modelling techniques essentially based on the solution of nested boundary value problems, one for each scale. The approach is based on the main assumption of periodic distribution of the

reinforcements at each scale and therefore the homogenization theory for periodic media is applied. At each scale the relevant representative volume (RV) is defined and modelled.

The proposed modelling is mainly implemented in a two-scale computational homogenization procedure to study the mechanical behaviour of textile composites ([2]) and multi-layer stitched composites ([3]). The first-scale homogenization deals with a yarn or a single layer considered as unidirectional fibre reinforced composite whose RV includes a single fibre and the surrounding matrix (RV size of the order 10^{-5} m). The second-scale homogenization regards a representative volume of the textile composite or of the multi-layer composite with homogenized yarns or layers respectively (RV size of the order 10^{-3} m).

The three-dimensional numerical procedure is developed to obtain the macroscopic constitutive law of the composite material i.e. the macroscopic stress-strain relationship. In order to follow the material behaviour up to failure, the numerical approach at the first-scale complies with von Mises and Hill criteria as failure domain of the matrix and fibre respectively, while in the second-scale the failure domain of the homogenized yarns is governed by Tsai-Hill failure theory for anisotropic materials. The progressive damage of the composite material is followed, during the analysis in the second-scale, by a procedure involving the stiffness matrix elements degradation. The elements of the stiffness matrix are reduced depending on the involved failure mechanism of the yarns (see e.g. [4]).

The experimental data on a glass textile plain weave composite and a multi-axial multi-ply carbon stitched laminate are compared to the results of the numerical simulations.

2 Theoretical background

The three-dimensional numerical procedure to study multi-axial composite materials is developed in the framework of the homogenization theory for periodic media [5].

The main hypotheses are: regular arrangement of the reinforcing fibres in the composites and a perfect link between fibres and matrix. The last hypothesis is a limitation and could be removed introducing interfaces at different scale levels to transmit forces between the fibres and the matrix.

The macroscopic mechanical behaviour of the composite material is described in term of macroscopic stress $\underline{\underline{\Sigma}}$ and macroscopic strain $\underline{\underline{E}}$, defined as volumetric averages of the relevant microscopic variables ($\underline{\underline{\sigma}}(\underline{x})$, $\underline{\underline{\epsilon}}(\underline{x})$) depending on the position vector \underline{x} in the representative volume (RV) (see Eq. 1, being V the RV volume) (double and single underlined symbols denote matrices and vectors respectively).

$$\underline{\underline{\Sigma}} = \frac{1}{V} \int_V \underline{\underline{\sigma}} dV; \quad \underline{\underline{E}} = \frac{1}{V} \int_V \underline{\underline{\epsilon}} dV \quad (1)$$

The multi-scale modelling technique proposed solves at each scale a homogenization problem to determine the macroscopic constitutive law $\underline{\underline{\Sigma}}-\underline{\underline{E}}$ at the current level. The problem to solve numerically is:

$$\text{div } \underline{\underline{\sigma}} = \underline{\underline{0}} \quad \text{in } V \quad (2a)$$

$$\underline{\underline{\sigma}} = F(\underline{\underline{\epsilon}}(\underline{u})) \quad \text{in } V \quad (2b)$$

$$\underline{\underline{u}} = \underline{\underline{u}} - \underline{\underline{E}} \cdot \underline{x} \quad V\text{-periodic} \quad (2c)$$

Eq. (2a) is the microscopic equilibrium equation; Eq. (2b) represents the microscopic constitutive law while Eq. (2c) is the periodic kinematics boundary condition.

In order to reproduce the periodicity of the heterogeneous material in terms of kinematics quantities by Eq. (2c), the following general relation of the displacement field holds:

$$\underline{u}(\underline{x}) = \underline{u}^0 + \underline{\underline{\Omega}} \cdot \underline{x} + \underline{\underline{E}} \cdot \underline{x} + \underline{\underline{u}}(\underline{x}) \quad (3)$$

where \underline{u}^0 represents a rigid displacement of the RV and $\underline{\underline{\Omega}}$ is the skew symmetric tensor related to the small rigid rotation of the RV. The pure strain modes of the RV are described by the last two terms in (3): a constant term (the macroscopic strain $\underline{\underline{E}}$)

and a V -periodic term, with zero average value, associated with the V -periodic part $\underline{\underline{u}}$ of the microscopic displacement field.

3 Finite element modelling

The main task to implement problem (2) in a displacement formulation finite element code is the assignment of the boundary conditions to ensure that the displacement field complies with Eq. (3).

In the following the incremental problem (2) is solved numerically at two scale levels to investigate the mechanical behaviour of textile composites and multi-layer stitched composites.

The first scale numerical modelling deals with the yarns of the reinforcing textile (first application) and the fibres in each layer (second application) both considered as unidirectional fibre reinforced composites. The second scale numerical modelling considers the RV of the textile composite material (first application) and the RV of the multi-layer stitched composite (second application) in which the yarns and the layers respectively are described through a homogenized material obtained by the first scale modelling.

In the following some details on the assignment of the boundary conditions to have the displacement field in Eq. (3) are detailed for both the two scale modelling.

3.1 First scale numerical modelling

The first scale concerns a yarn or a lamina. They are considered as unidirectional fibre reinforced composites (see Fig. 1a). Their mechanical properties are obtained by means of the finite element model of a representative volume. Assuming the fibres arranged according to a regular hexagonal pattern, the representative volume employed has the shape in Fig. 1b.

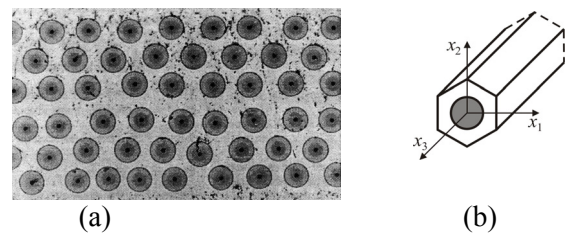


Fig. 1. (a) periodic unidirectional fibre reinforced composite; (b) representative volume (RV).

The 3D finite element model of the RV comprises the material between two sections perpendicular to the fibre axis x_3 (Fig. 1b). The problem symmetries allow studying only half of the RV. The mesh used in the analyses is shown in Fig. 2 (more details in [6]).

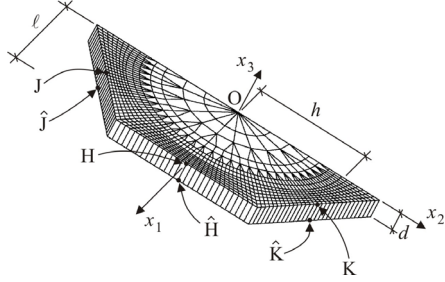


Fig. 2. Finite element mesh of the representative volume (RV) in the first scale modelling.

The boundary conditions ensuring the displacement field to be of the form (3) can be written as detailed in [6] according to the FE mesh in Fig. 2. Moreover, to avoid rigid rotations of the RV the macroscopic displacement gradient $\underline{\Psi} = \underline{\Omega} + \underline{E}$ must be symmetric. This implies the skew symmetric part $\underline{\Omega}$ to vanish and as consequence the six independent components of \underline{E} can be explicitly written in term of six free nodal displacement components as obtained in [6].

3.2 Second scale numerical modelling

The second scale concerns a textile composite material and a multi-layer stitched composite in which the yarns and the layers respectively are described through a homogenized material, obtained by the first scale modelling, equivalent from the mechanical point of view to the real one.

The representative volume RV of the considered materials involves the homogenized yarns and the surrounding matrix or the homogenized layers in the multi-layer stitched composite according to stacking sequence.

In the following, the displacement boundary conditions to reproduce the periodicity of the considered materials are detailed for the textile composite RV only ([2]). The same boundary conditions can be applied to the RV of the multi-layer stitched composite (see [3]).

According to the periodic geometry of the plane weave textile composite material considered,

the sketch of its RV, including the FE mesh of the reinforcement, is in Fig. 3.

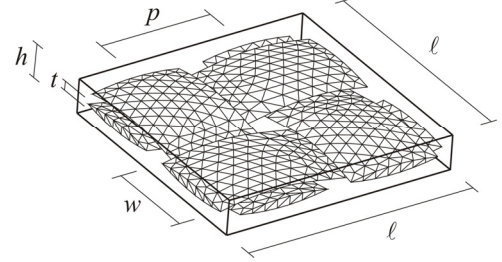


Fig. 3. Representative volume (RV) of the textile plane weave composite material. FE mesh of the reinforcement.

The periodic displacement boundary conditions applied in the second scale level are defined according to Eq. 2c. Referring to the external geometry of the RV singled out from a textile composite in Fig. 4, such conditions can be written as:

$$\underline{u}_J - \underline{u}_Y = \underline{E}(\underline{x}_J - \underline{x}_Y) \quad (4a)$$

$$\underline{u}_H - \underline{u}_K = \underline{E}(\underline{x}_H - \underline{x}_K) \quad (4b)$$

In Eq. (4a) J and Y are two points on the cross sections $x_1 = \ell/2$ and $x_1 = -\ell/2$ corresponding in the periodicity; in Eq. (4b) H and K are two points on the cross section $x_2 = \ell/2$ and $x_2 = -\ell/2$ corresponding in the periodicity (see Fig. 4).

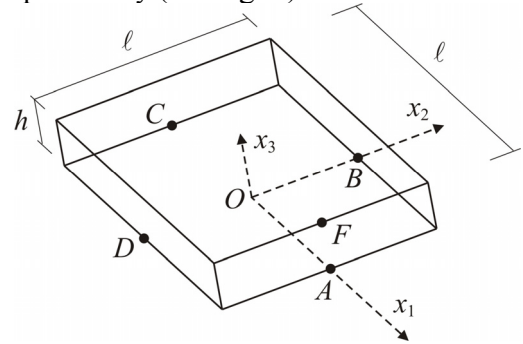


Fig. 4. Characteristic points of the RV finite element model.

Accounting for the general expression of the displacement field Eq. (3) and the periodicity condition Eq. (4), the macroscopic displacement gradient in the plane x_1 - x_2 becomes:

$$\underline{\Psi} = \underline{\Omega} + \underline{E} = \begin{bmatrix} \frac{u_1^A - u_1^C}{\ell} & \frac{u_1^B - u_1^D}{\ell} \\ \frac{u_2^A - u_2^C}{\ell} & \frac{u_2^B - u_2^D}{\ell} \end{bmatrix} \quad (5)$$

where (A, C) and (B, D) are the midpoints pairs corresponding in the periodicity (Fig. 4).

Rigid translations of the model are suppressed by prescribing $\underline{u}^0 = \underline{0}$ (see Fig. 4). Rigid rotations can be avoided by imposing the skew symmetric tensor $\underline{\underline{\Omega}}$ to vanish [2].

As consequence, the components of the symmetric tensor \underline{E} in the plane x_1 - x_2 can be explicitly written as:

$$E_{11} = \frac{u_1^A - u_1^C}{d_1} \quad (6a)$$

$$E_{22} = \frac{u_2^B - u_2^D}{d_2} \quad (6b)$$

$$E_{12} = \frac{u_2^A - u_2^C}{\ell} \quad (6c)$$

In the numerical simulations macroscopic strain components are prescribed according to Eq. (6) and the macroscopic stress tensor is evaluated by the volumetric average (1a) of the microscopic counterparts in the Gauss integration points.

3.3 Failure criteria

In order to obtain the complete mechanical behaviour up to failure of the composite materials investigated, the failure criteria to employ in the numerical modelling must be defined.

In the first scale modelling the von Mises and the Hill failure behaviours for the fibres and matrix respectively were considered.

In the second scale modelling the progressive damage of the composite materials is studied assuming the Tsai-Hill failure domain for the anisotropic homogenized yarns or layers while the isotropic matrix complies with von Mises criterion. The strength parameters of the homogenized materials for Tsai-Hill domain are evaluated by the finite element model in the first scale.

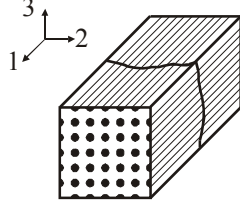
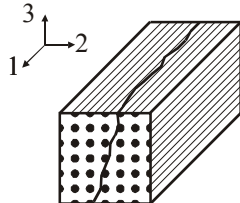
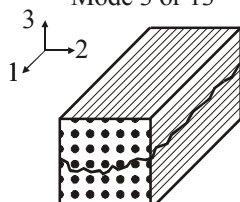
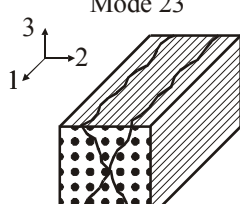
To simulate the progressive damage up to a complete failure of the homogenized materials a degradation procedure is implemented in the finite element code. When the average stress state in a finite element satisfies the assumed failure criterion its stiffness matrix elements are dropped down according to the failure mechanism involved. The

failure mechanics taken into consideration comply with the proposal in [4].

The four possible damage modes are depicted in Table 1. Mode 1 represents the fibre breakage (being 1 the fibre direction). Modes 2 and 3 are due to transverse failure by normal stress. Modes 13, 23, 12 simulate shear cracking.

The activation of a failure mode is assumed to depend on the maximum stress-strength ratio. The link between damage modes and stress-strength ratios is detailed in Table 1 where F^t , F^c , F^s are the tensile, compressive and shear homogenized strength parameters (in the numerical analyses is assumed $F^t = F^c$).

Table 1. Damage modes and maximum stress-strength ratio correlation.

Damage mode	Maximum stress-strength ratio
Mode 1 	$\frac{\sigma_1^2}{F_1^t F_1^c}$
Mode 2 or 12 	$\frac{\sigma_2^2}{F_2^t F_2^c}$ or $\left(\frac{\tau_{12}}{F_{12}^s}\right)^2$
Mode 3 or 13 	$\frac{\sigma_3^2}{F_3^t F_3^c}$ or $\left(\frac{\tau_{13}}{F_{13}^s}\right)^2$
Mode 23 	$\left(\frac{\tau_{23}}{F_{23}^s}\right)^2$

The components of the stiffness matrix to be reduced depend on the active damage mode. In Table 2 the reduction schemes associated to each damage mode are described. The damage parameter d is assumed equal to 0.01.

Table 2. Reduced stiffness matrix depending on the active damage mode.

Damage mode	Reduced stiffness matrix
Mode 1	$\begin{bmatrix} dQ_{11} & dQ_{12} & dQ_{13} & 0 & 0 & 0 \\ & Q_{22} & Q_{23} & 0 & 0 & 0 \\ & & Q_{33} & 0 & 0 & 0 \\ & sym. & & dQ_{44} & 0 & 0 \\ & & & & dQ_{55} & 0 \\ & & & & & Q_{66} \end{bmatrix}$
Mode 2 or 12	$\begin{bmatrix} Q_{11} & dQ_{12} & Q_{13} & 0 & 0 & 0 \\ & dQ_{22} & dQ_{23} & 0 & 0 & 0 \\ & & Q_{33} & 0 & 0 & 0 \\ & sym. & & dQ_{44} & 0 & 0 \\ & & & & Q_{55} & 0 \\ & & & & & dQ_{66} \end{bmatrix}$
Mode 3 or 13	$\begin{bmatrix} Q_{11} & Q_{12} & dQ_{13} & 0 & 0 & 0 \\ & Q_{22} & dQ_{23} & 0 & 0 & 0 \\ & & dQ_{33} & 0 & 0 & 0 \\ & sym. & & Q_{44} & 0 & 0 \\ & & & & dQ_{55} & 0 \\ & & & & & dQ_{66} \end{bmatrix}$
Mode 23	$\begin{bmatrix} Q_{11} & dQ_{12} & dQ_{13} & 0 & 0 & 0 \\ & dQ_{22} & dQ_{23} & 0 & 0 & 0 \\ & & dQ_{33} & 0 & 0 & 0 \\ & sym. & & dQ_{44} & 0 & 0 \\ & & & & dQ_{55} & 0 \\ & & & & & dQ_{66} \end{bmatrix}$

4 Applications and comparisons

The numerical procedure is applied to simulate the tensile mechanical behaviour of a glass fibres

balanced plane weave textile composite and a multi-axial multi-ply carbon stitched laminate.

The numerical results are compared to the experimental data. The mechanical properties of glass fibres textile composite were determined by experimental characterisation carried out by the author and co-workers, while the experimental tests on the multi-axial multi-ply carbon stitched laminate are detailed in [1].

4.1 Glass fibres plane weave textile composite

The mechanical properties of the textile composite components (glass fibres and epoxy resin) are in Table 3.

The periodic geometry in the laminate plane of the considered textile composite is reproduced by the RV shape drawn in Fig. 3 according to the geometric input detailed in Table 4. In Table 4 the packing density of the yarns (p_d) and the fibre volume fraction (c_f) are reported. The elliptical shape of the cross-section and the longitudinal heart line of the yarns were reproduced on the basis of microscopic investigations [2].

Table 3. Mechanical properties of the textile composite components.

	Glass Fibres	Epoxy Matrix
Young modulus [MPa]	76000	2520
Poisson ratio	0.22	0.35
Tensile strength [MPa]	2000	50

Table 4. Geometric features of the RV for the glass fibres plane weave textile composite (see Fig. 3).

ℓ [mm]	t [mm]	w [mm]	p [mm]	h [mm]	p_d [%]	c_f [%]
3.3	0.155	1.48	1.64	0.33	83	50.6

The first numerical step, regarding the yarns as unidirectional composites, was carried out assuming the hexagonal pattern of the fibres (Fig. 2) and taking the packing density of the yarns as fibre volume fraction. The numerical analyses provided the elastic and the strength properties of the homogenized transversally isotropic yarns reported in Table 5, according to the reference axes in Fig. 2.

In the second numerical step, the finite element mesh of the textile composite RV consists of homogenized yarns having the mechanical

properties (Table 5) obtained in the first step surrounded by the epoxy resin (see Fig. 3 for the mesh of the homogenized yarns).

The results of the second numerical modelling are compared to the experimental data in Fig. 5 in terms of the macroscopic tensile stress-strain relationship. The numerical global response of the textile composites is stiffer than the experimental, even if the failure stress agrees with the experiment. This is probably due to an overestimation of the fibre volume fraction of the composite.

Table 5. Mechanical properties of the transversally isotropic homogenized yarns (first scale modelling).

$E_1=E_2$ [MPa]	23160
E_3 [MPa]	63500
ν_{12}	0.31
$\nu_{13}=\nu_{23}$	0.23
G_{12} [MPa]	8446
$G_{13}=G_{23}$ [MPa]	8821
$F_1^t = F_2^t$ [MPa]	179
F_3^t [MPa]	1672

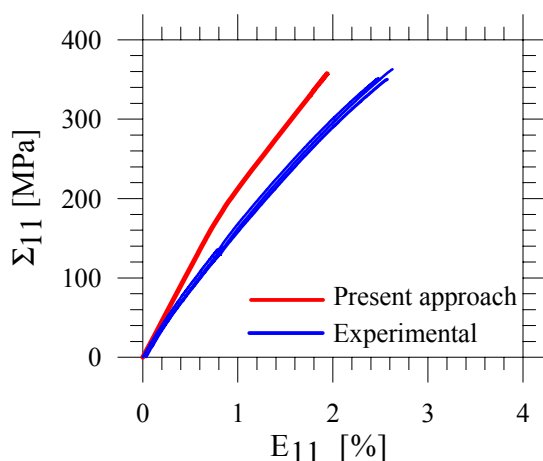


Fig. 5. Macroscopic stress-strain behaviour by the present approach and experiments for the glass fibres plane weave textile composite.

4.2 Multi-axial multi-ply carbon stitched laminate

A quadriaxial carbon laminate with stacking sequence $(45^\circ/90^\circ/-45^\circ/0^\circ/0^\circ/-45^\circ/90^\circ/45^\circ)_s$, experimentally investigated in [1], is considered.

The numerical procedure was applied to predict the complete behaviour up to failure of the quadriaxial laminate without stitching and including the channels produced by stitching.

The mechanical properties of the unidirectional plies were computed in the first scale homogenization, assuming the fibre volume fraction equal to 44% and the properties of carbon fibre and resin matrix reported in [1]. The obtained numerical results are in Table 6, according to the reference axes in Fig. 2.

Table 6. Mechanical properties of the transversally isotropic homogenized plies (first scale modelling).

$E_1=E_2$ [GPa]	72
E_3 [GPa]	238
ν_{12}	0.30
$\nu_{13}=\nu_{23}$	0.27
G_{12} [GPa]	28
$G_{13}=G_{23}$ [GPa]	86
$F_1^t = F_2^t$ [MPa]	1777
F_3^t [MPa]	3950

The second scale homogenization was performed at the multi-ply composite level taking into consideration the homogenized layers from the first-scale analyses. The RV geometry of the quadriaxial multi-ply composite with stitching channels complies with the geometry of the plies and of the stitching measured and detailed in [7]. The FE mesh of the RV employed to perform numerical analyses is depicted in Fig. 6. The transversal stitching channels (along axis 2, see Fig. 6) are considered filled by the matrix material, while the channels in the plane 1-3 and the stitching fibres are not taken into consideration.

The tensile numerical simulations in direction 1 (see Fig. 6) provide the results depicted in Fig. 7. The numerical macroscopic stress-strain relations are above (perfect laminate without channels) and below (with stitching channels) the experimental tests respectively. The numerical model with

stitching channels predicts a constitutive behaviour of the laminate close to the experimental one both in term of elastic stiffness and ultimate failure.

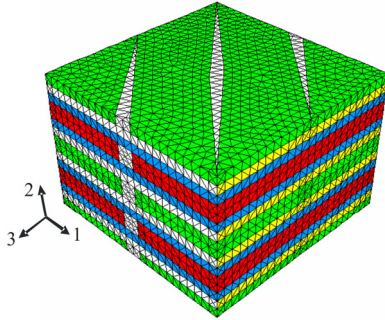


Fig. 6. Quadriaxial carbon stitched laminate. FE model of the RV with transversal channels.

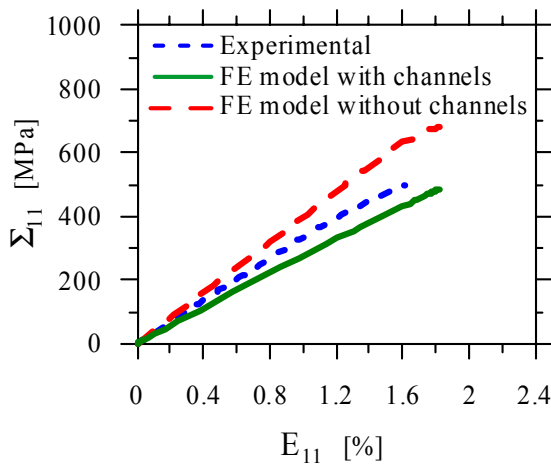


Fig. 7. Macroscopic stress-strain behaviour by the present approach and experiments for the multi-axial multi-ply carbon stitched laminate.

5 Conclusions

An overview of a numerical approach to evaluate the mechanical behaviour until failure of multi-axial composites and the validation of the method against experiments was presented.

The procedure is a multi-scale modelling technique essentially based on the solution of nested boundary value problems, one for each scale.

The main assumption at each scale is the periodic distribution of the reinforcements.

The proposed three-dimensional modelling is implemented in a two-scale computational homogenization procedure. The first scale involves a unidirectional fibre reinforced composite. The second scale takes into consideration the geometry

of the multi-axial reinforcement having the homogenized mechanical properties from the first-scale analyses.

The numerical procedure was applied to predict the mechanical behaviour up to failure of a glass textile plain weave composite and a multi-axial multi-ply carbon stitched laminate. In both cases the numerical results are compared to the available experimental investigations.

The accuracy of the numerical procedure in the simulation of the mechanical behaviour of the considered composite materials is satisfactory in the elastic and ultimate ranges, in spite of the initial periodicity hypothesis.

In conclusion, it should be underlined that the proposed procedure was implemented into a commercial finite element code and therefore appears to be an efficient tool for industrial applications.

6 References

- [1] Thanh T.C., Vettori M., Lomov S., Verpoest I., "Carbon composites based on multi-axial multi-ply stitched preforms. Part 4. Mechanical properties of composites and damage observation", *Composites Part A*, Vol. 36, pp. 1207-1221, 2005.
- [2] Carvelli V., Poggi C., "A homogenization procedure for the numerical analysis of woven fabric composites". *Composite Part A*, Vol. 32, pp. 1425-1432, 2001.
- [3] Carvelli V., Poggi C., "A numerical model for the mechanical properties of multi-axial multi-ply stitched fabric composites", *Proceeding of the 7th International Conference on Textile Composites TEXCOMP 7*, Yonezawa Yamagata (Japan), 2004.
- [4] Zako M., Uetsuji Y., Kurashiki T., "Finite element analysis of damaged woven fabric composite materials", *Composite Science and Technology*, Vol. 63, pp. 507-516, 2003.
- [5] Suquet P., "Elements of homogenization for inelastic solid mechanics". In E. Sanchez-Palencia and A. Zaoui eds. 'Homogenization techniques for composite media', Lecture Notes in Physics 272, Springer, Wien, pp. 193-278, 1985.
- [6] Carvelli V., Taliercio A., "A micromechanical model for the analysis of unidirectional elastoplastic composites subjected to 3D stresses", *Mechanics Research Communications*, Vol. 26, pp. 547-553, 1999.
- [7] Lomov S.V., Belov E.B., Bischoff T., Ghosh S.B., Thanh T.C., Verpoest I., "Carbon composites based on multi-axial multi-ply stitched preforms - Part 1: Geometry of the perform", *Composites Part A*, Vol. 33, pp. 1171-1183, 2002.